

# A simple and sensitive assay for ampicillin in pharmaceuticals using gold nanoparticles as spectroscopic probe reagent

Ghodratollah Absalan · Abdolkarim Abbaspour ·  
Marzieh Jafari · Mohsen Nekoeinia · Hamid Ershadifar

Received: 12 June 2014 / Accepted: 18 October 2014 / Published online: 31 October 2014  
© Iranian Chemical Society 2014

**Abstract** A novel kinetic spectrophotometric method is developed for determination of ampicillin. The method is based on aggregation of gold nanoparticles in a chemical process that involved decomposition of ampicillin catalyzed by cadmium ion in methanol as solvent. The optimum experimental conditions for determination of ampicillin were established. The method permitted determination of ampicillin in a concentration range of 16.0–96.0  $\mu\text{g ml}^{-1}$  with a detection limit of 13.0  $\mu\text{g ml}^{-1}$ . The interferences of the species which are mostly available in biological samples were not significant in determination of ampicillin. The method is simple and sensitive for analyzing of ampicillin and is applicable for its assay in pharmaceutical formulations.

**Keywords** Gold nanoparticle · Ampicillin · Spectrophotometry · Cadmium ion · ICH guideline

## Introduction

In nature, the antibiotics are synthesized by living organisms that kill or stop the growth of other microorganisms. In biological science, the interest in analysis of antibiotics arises from the fact that they are responsible for the appearance of bacterial strains that are resistant to antibiotics which are important drugs for the treatment of many serious infectious diseases and thus antibiotic's determination

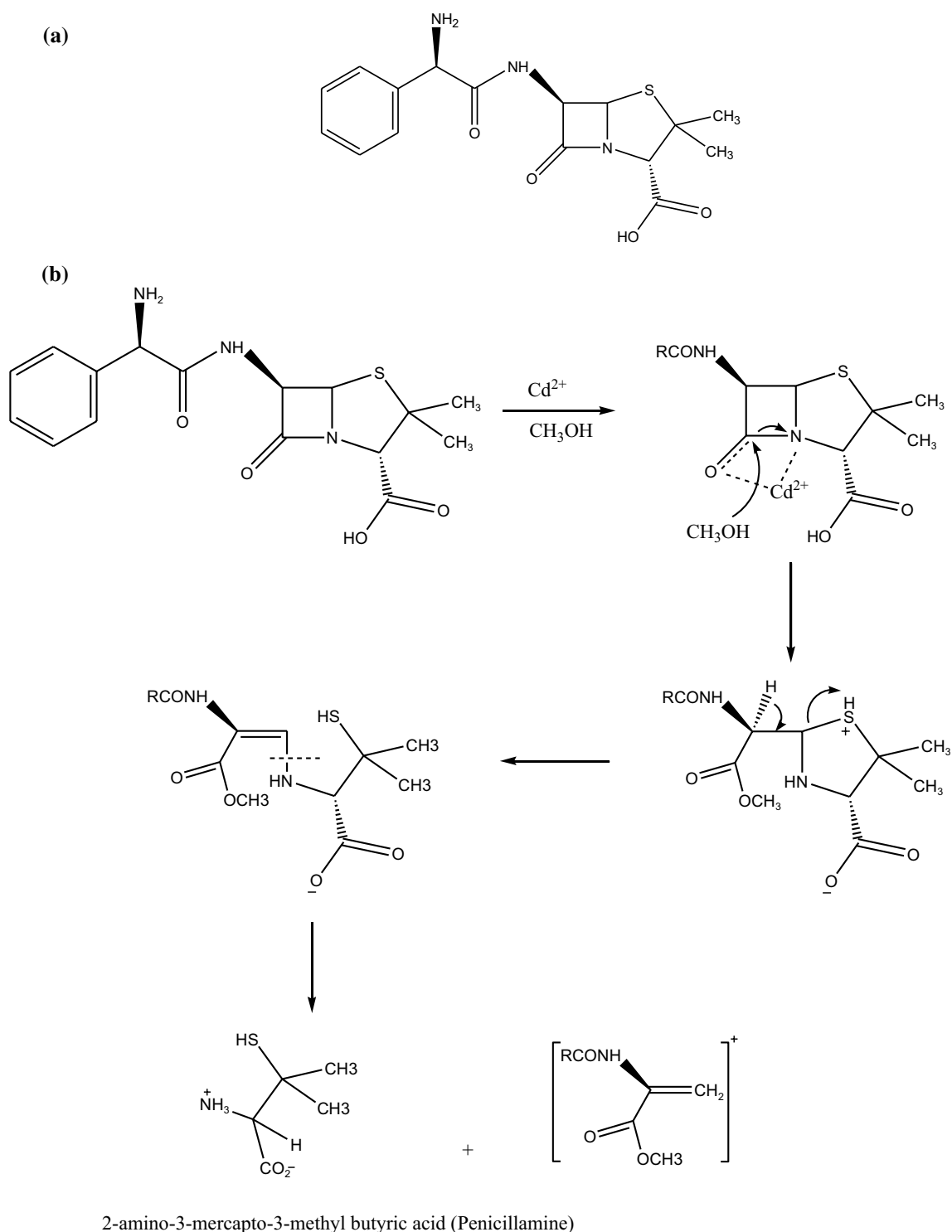
is important [1]. The first antibiotic was penicillin that discovered in 1928 from a mold culture. All penicillins are  $\beta$ -lactam antibiotics. A  $\beta$ -lactam is a ring with a heteroatomic structure, consisting of three carbon atoms and one nitrogen atom [2].

Ampicillin (6-[(aminophenyl acetyl) amino]-3,3-dimethyl-7-oxo[2 s-2 $\alpha$ ,5 $\alpha$ ,6 $\beta$  (S\*)]), Scheme 1a, is one of the important  $\beta$ -lactam antibiotic used to treat or prevent gram-negative bacteria and bacterial infections. The nature of ampicillin is acidic, and it inhibits the protein synthesis. The antibacterial and pharmacological properties of ampicillin are determined by side chain of this compound [3]. Ampicillin is used to treat some diseases such as Enterococcal endocarditis, Meningitis, etc. Ampicillin also inhibits the synthesis of bacterial cell wall and leads to cell lysis [4]. Because of its high activity, low toxicity and acid stability, ampicillin is commonly used in medical treatments [5]. In view of its pharmacological importance, considerable work has been done for its chemical analysis. Analytical methods for determination of ampicillin, in biological and pharmaceutical samples, employ techniques such as chromatography [6–9], spectrophotometry [10–13], spectrofluorimetry [14], near-infrared spectroscopy [15, 16], mass spectrometry [17, 18] and NMR spectroscopy [19, 20]. Chromatography, mass spectrometry and NMR methods are expensive and time-consuming and require expertise.

Spectrophotometric techniques provide practical and significant economic advantages over other methods; therefore, they are the best choice for pharmaceutical analysis [21, 22]. However, most pharmaceutical drugs have strong absorption bands in the range of ultraviolet and, therefore, could interfere with determination of ampicillin. Using of chromogenic or fluorogenic agent in spectroscopy is a common approach used to solve the above-mentioned problem. Recently, chromogenic agents based on aggregation

G. Absalan (✉) · A. Abbaspour · M. Jafari · H. Ershadifar  
Professor Massoumi Laboratory Department of Chemistry  
College of Sciences, Shiraz University, 71454 Shiraz, Iran  
e-mail: gubsulun@yahoo.com; absalan@susc.ac.ir

M. Nekoeinia  
Department of Chemistry, Payame Noor University,  
19395-4697 Tehran, Iran



**Scheme 1** **a** Ampicillin chemical structure, **b** Degradation of ampicillin in alcoholic media

of metallic nanoparticles through changes in color have received considerable attention because of their simplicity, high sensitivity and low cost [23].

In recent years, gold nanoparticles (AuNPs) have attracted great interest due to their unique properties such

as unusual catalytic, electronic, optical and thermal properties, as well as high stability, biological compatibility, controllable morphology, size dispersion and easy surface functionalization [24]. Gold nanoparticles are known for their beautiful wine-red coloration and are known to

have one of the highest extinction coefficients ( $10^5$ – $10^8$  L mol<sup>-1</sup>cm<sup>-1</sup>) [25]. The bright color of nanoparticles is ascribed to the transverse oscillations of the surface electrons of the particle on interaction with light of a suitable wavelength, the phenomena is called surface plasmon resonance (SPR). It has been shown that the surface plasmon band is greatly dependent on the diameter and shape of gold nanoparticles and their interaction with medium [26]. In nanobiotechnology, AuNPs are used in recognizing biomolecules attached to their surface by means of physical adsorption or coupling through the Au–S dative bond [27]. This makes them promising tool in colorimetric sensors for specific target detection. Aggregation of gold nanoparticles leads to a change in their optical properties (i.e., a red shift in surface plasmon, or a red to blue color change as detected by the naked eye), which can be used in the colorimetric detection of target agents [28].

So far many gold nanoparticle-based assays have been reported and summarized in reviews [29–33]. In this work, AuNPs is proposed as a chromogenic agent for determination of ampicillin in pharmaceutical samples. The idea is based on the Cd<sup>2+</sup>-catalyzed decomposition of ampicillin in methanol. One of the degradation products of the chemical process is 2-amino-3-mercapto-3-methyl butyric acid, that its –SH group induces the aggregation process of the gold nanoparticles [34]. This aggregation leads to a decrease in absorption of AuNPs around the wavelength of 528 nm along with wavelength shift to 670 nm.

## Experimental

### Apparatus

The UV–Vis absorbance spectra were collected using an Ultrospec 4000 (Pharmacia Biotech, UK) spectrophotometer, with matched 10-mm quartz cells (Helma cell) and a scan rate of 2500 nm min<sup>-1</sup>. The Quartz cells were thermostated at 25.0 °C by an exterior circulation forced into the cell-holder from a thermostated bath (Huber, Germany). The pH measurements were performed with a Metrohm model 780 pH-meter using a combined glass electrode.

The FTIR spectra of gold nanoparticles in aqueous solution are recorded using an FTIR spectrometer (spectrum RXI, PerkinElmer) equipped with CaF<sub>2</sub> circular cell windows. The TEM micrographs of the colloidal dispersion and aggregation were obtained by a transmission electron microscope (Zeiss, model EL10C) operated at an accelerating voltage of 80 kV. The XRD patterns of the prepared samples were acquired with a Bruker D8 Advance X-ray diffractometer using Cu K<sub>α</sub> radiation (40 kV, 300 mA) of wavelength 0.154 nm and interpreted with X'Pert High-Score software to confirm the structure of the materials.

Samples for XRD characterization were prepared by dropwise placing of the as-prepared colloidal gold samples on a plexiglass sheet followed by drying at room temperature.

### Materials

Pure ampicillin trihydrate was kindly supplied by Farabi Pharmaceutical Company (Isfahan, Iran). Methanol with a synthetic grade (p.a., >99.5 %, Merck) was used in all experiments. Stock solution of ampicillin with concentration of  $1.0 \times 10^{-2}$  mol L<sup>-1</sup> was prepared by dissolving 0.2017 g ampicillin trihydrate in a 50-ml volumetric flask and was diluted to the mark with doubly distilled water. It should be mentioned that the manufacturer had reported that this solution is stable at least for 2 weeks at 4.0–8.0 °C. The stock solution of Cd<sup>2+</sup> with concentration of 0.10 mol L<sup>-1</sup> was prepared by dissolving 0.7712 g Cd(NO<sub>3</sub>)<sub>2</sub>·4H<sub>2</sub>O (Merck) into a 25-ml volumetric flask and was diluted with water to the mark. Other solutions of Cd<sup>2+</sup> were prepared by diluting suitable amount of the stock solution with acetate buffer. Acetate buffer solution ( $5.0 \times 10^{-2}$  mol L<sup>-1</sup>) was prepared by dissolving appropriate amount of CH<sub>3</sub>COONa·3H<sub>2</sub>O (Interchem) in doubly distilled water. The pH was adjusted by addition of appropriate amounts of concentrated HCl solution to cadmium solution that was already contained acetate buffer.

### Synthesis of gold nanoparticles

Several procedures for preparation of gold nanoparticles have been reported [35–37]. Due to high yield and simplicity, the most commonly used method for preparation of colloidal gold nanoparticles is the citrate reduction method which also was used in this work. For the synthesis of gold colloids, 50.0 ml HAuCl<sub>4</sub> (0.010 %w/w) solution was heated up to its boiling point. While stirring vigorously, 750 μL Na<sub>3</sub>C<sub>6</sub>H<sub>5</sub>O<sub>7</sub>·2H<sub>2</sub>O (1.0 %w/w) was added rapidly and the solution was maintained at boiling point for 30 min until appearance of a red color. After removing the heating source, the solution was continuously stirred for about 15 min to reach the room temperature. The produced nanoparticles were eventually stored at 4.0 °C. Based on a similar procedure used for synthesis of gold nanoparticles [38], the size of the nanoparticles was expected to be 25 nm. For calculating the concentration of the nanoparticles [39], a size of 25 nm was considered showing that nanoparticles had a concentration of  $5.267 \times 10^{-10}$  mol L<sup>-1</sup>.

### Procedure for ampicillin determination

Aliquots of 1.0 ml methanol, 1.0 ml gold nanoparticles and 500 μl Cd<sup>2+</sup> solution ( $5.0 \times 10^{-4}$  mol L<sup>-1</sup> with a pH adjusted at 4.6) were added into a quartz cell. The change

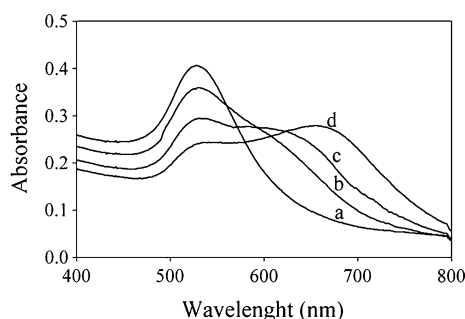


**Fig. 1** Variation of absorbance spectra of gold nanoparticles with ampicillin concentrations of: **a** 0.0; **b** 16; **c** 32; and **d** 56  $\mu\text{g ml}^{-1}$ . Reaction conditions were pH of 4.6 with  $C_{\text{Cd}^{2+}} = 5.0 \times 10^{-4} \text{ mol L}^{-1}$  at 25 °C

in absorption of this solution was followed with injection of a sample solution containing ampicillin at 670 nm which is the wavelength that was selected from the absorption spectra of gold nanoparticles in the presence of ampicillin as shown in Fig. 1. The reaction rate was measured spectrophotometrically by monitoring the increase in absorbance of the reaction mixture using fixed-time method. The absorption changes,  $\Delta A$  ( $\Delta A = A_{1000} - A_{100}$ , where  $A_{100}$  and  $A_{1000}$  refer to absorbance measurements taken at 100 and 1000 s at 670 nm, respectively), were followed after starting the reaction.

#### Determination of ampicillin in pharmaceutical formulation

Three capsules of different pharmaceutical companies (Dana Pharmaceutical Co., Cosar Co. and Farabi Pharmaceutical Co., Iran) were prepared and were analyzed using the proposed method. A quantity equivalent to 500 mg drug, from a mixed contents of 10 capsules, was accurately weighed and was transferred into a 100-ml volumetric flask. The sample was dissolved in double-distilled water

and was sonicated for 30 min with an Ultrasonic cleaner model CD-4800 (China) in room temperature. The content of the flask was filtered and 1.0 ml of the filtrate was pipetted into a 10-ml volumetric flask and was diluted up to the mark with double-distilled water.

## Results and discussion

### Characterization of gold nanoparticles

The UV–vis spectroscopy is usually first evidence to identify the formation and optical properties of gold nanostructure. As shown in Fig. 1a, the synthesized AuNPs exhibited a surface plasmon resonance band in 528 nm. The TEM image obtained for colloidal gold nanoparticles is shown in Fig. 2a. From this image, it is clear that the surface morphology of the synthesized AuNPs was almost spherical and that the average size of the nanoparticles was about  $25 \pm 2 \text{ nm}$ . Also, the TEM image of the aggregated gold nanoparticles is shown in Fig. 2b. The crystalline structure of the AuNPs was confirmed using X-ray diffraction analysis. The XRD pattern of the nanoparticles is shown in Fig. 3. The Bragg reflections peaks that appeared at  $38.2^\circ$ ,  $44.5^\circ$ ,  $64.6^\circ$  and  $78.2^\circ$ , respectively, can be assigned to (111), (200), (220) and (311) crystalline plane diffraction peaks of face-centered cubic (fcc) phase of gold [40].

### Mechanism of the reaction

There are a lot of theoretical and experimental researches for alcoholysis reaction with  $\beta$ -lactam antibiotics [34, 41, 42]. In alcoholic media, the  $\beta$ -lactam bond of ampicillin is broken and the hydroxylic hydrogen atom migrates to the nitrogen atom of  $\beta$ -lactam amide (Scheme 1b) [43]. Garcia et al. [34] showed that the decomposition of ampicillin in methanol medium is catalyzed by  $\text{Cd}^{2+}$ . They proposed

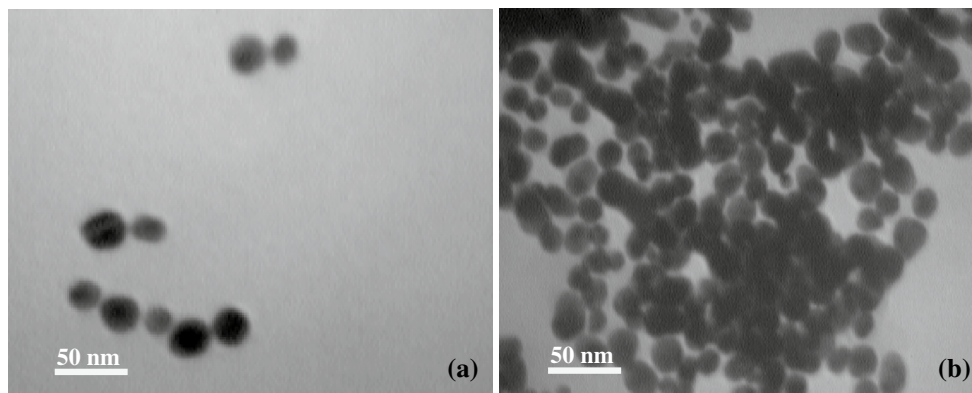


**Fig. 2** The TEM image of nanoparticles: **a** after synthesis; **b** in the presence of ampicillin in methanol

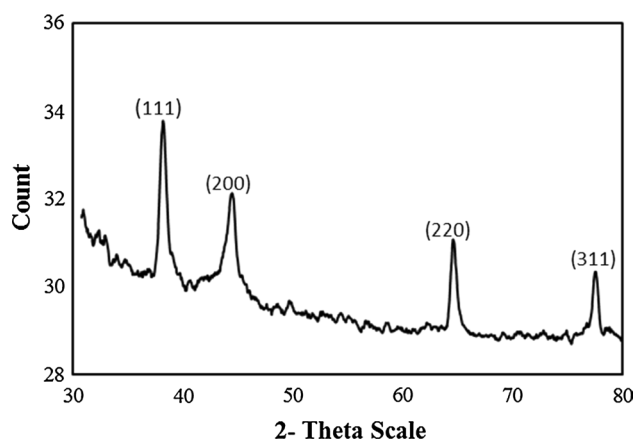
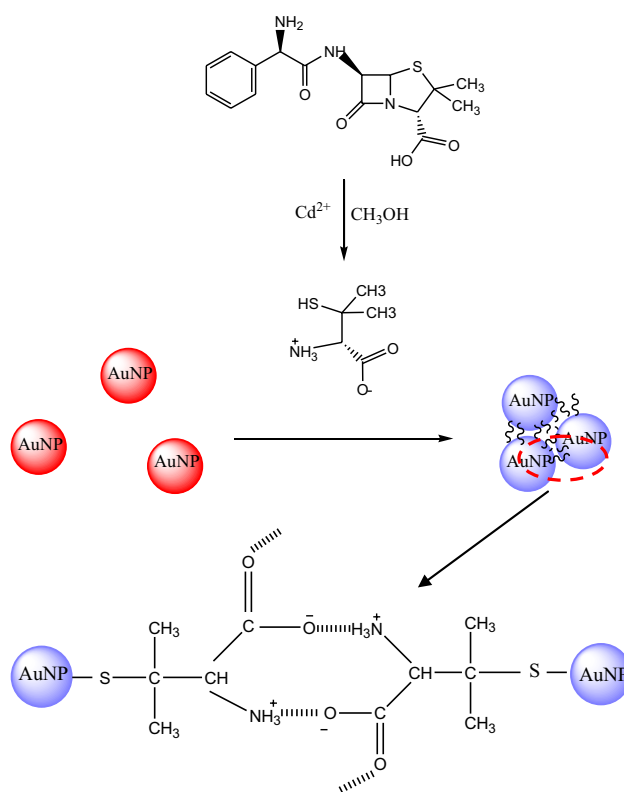


**Fig. 3** The XRD patterns of the gold nanoparticles

that methanol molecules may involve in a nucleophilic attack to  $\beta$ -lactam carbonyl group of ampicillin molecule which facilitates the arrangement of the cadmium ions toward ampicillin molecules. The metal ion increases the electrophilicity of the carbonyl carbon and also the bond-breaking step. The function of the cadmium (II) ion may be regarded as stabilization of the amine anion leaving group thus increasing the rate of carbon–nitrogen bond fission. One of the degradation products is 2-amino-3-mercapto-3-methyl butyric acid or penicillamine that contains  $-\text{SH}$  group. Penicillamine can bind to surface of gold nanoparticles by its thiol ( $-\text{SH}$ ) group [44]. This bond is formed due to the ligand-exchange reaction between penicillamine and citrate-capped gold nanoparticles. A possible model illustrating both penicillamine binding to gold nanoparticles and their aggregation is shown in Scheme 2 [45, 46]. While penicillamine adsorption on the surface of gold nanoparticles occurs through its thiol group, the adjacent nanoparticles could interact with each other through their carboxylic and amine groups which results in the aggregation of the particles. This could occur when the pH is adjusted. Besides the electrostatic interaction mechanism between amine and carboxylic groups, a possible formation of hydrogen bonds between surface-bonded penicillamine molecules is also reported [47].

To support this reaction, ampicillin-induced aggregation kinetics of gold nanoparticles was monitored by UV–Vis absorption spectra as shown in Fig. 4. Before adding ampicillin, gold nanoparticles showed a surface plasmon band at 528 nm whose intensity was decreased by addition of ampicillin accompanied by a marked increase in absorbance around 670 nm and a color change from red to blue. It is noted that the absorbance at 670 nm was increased with time. The inset of Fig. 4 shows the absorption of gold nanoparticles as a function of time. It is well known that such spectral changes in the surface plasmon band result from



**Scheme 2** Aggregation of gold nanoparticle in the presence of ampicillin

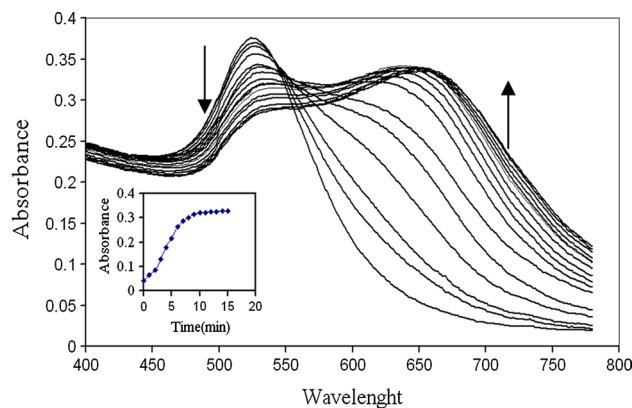


**Fig. 4** Absorbance spectra of gold nanoparticles in the presence of ampicillin and  $\text{Cd}^{2+}$  with different time. Reaction conditions were pH 4.6, temperature  $25^\circ\text{C}$ ,  $C_{\text{Amp}} = 56 \mu\text{g ml}^{-1}$ ,  $C_{\text{Cd}^{2+}} = 5.0 \times 10^{-4} \text{ mol L}^{-1}$ . Inset: the absorption at 670 nm of the gold nanoparticles as a function of time

plasmon coupling caused by the aggregation of gold nanoparticles. Thus, it was concluded that the spectral change in Fig. 4 would be caused by formation of gold nanoparticle aggregates induced by the alcoholysis product of ampicillin. Also, FTIR technique would be a reliable method for following the variations in the functional groups. The FTIR

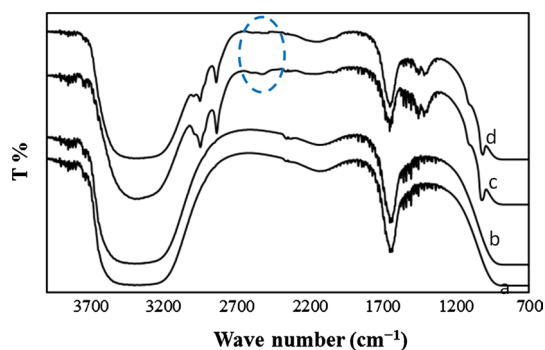


**Fig. 5** The FTIR spectra of: AuNPs (a), ampicillin solution (b), ampicillin degraded in the presence of methanol and Cd<sup>2+</sup> (c), and AuNPs in the presence of ampicillin in methanol and Cd<sup>2+</sup> (d)

bands seen in Fig. 5 are identified as follows. The bands observed at 1636 and 3350 cm<sup>-1</sup> indicate the stretching of –OH in water (Fig. 5a, b). When ampicillin degraded, two bands can be observed at 2873 cm<sup>-1</sup> and 2932 cm<sup>-1</sup>, corresponding to –CH<sub>2</sub>– vibration. Also, a weak band at about 2550 cm<sup>-1</sup> can be found confirming the presence of –SH group in the solution (Fig. 5c) which is caused by the degradation product (penicillamine) [48]. This band was not observed in the spectra of ampicillin in the presence of gold (Fig. 5d); confirming the Au–S interaction. Other bands remain unchanged.

#### Effect of variables on the reaction rate

In order to find the optimum experimental conditions for determination of ampicillin, the effect of solvent, pH, concentration of the reagents, temperature and ionic strength of the sample solution were examined.

#### Effect of solvent

The effect of solvent type on the reaction rate has been investigated systematically. The reaction was repeated in different solvents such as water, methanol, ethanol and propanol. It seems that the size and/or viscosity of the solvent molecules could be important parameters to be investigated for studying the kinetic of the process. The highest reaction rate was achieved when methanol was used as solvent; therefore, it was selected for the next investigations (Fig. 6).

#### Effect of Cd<sup>2+</sup> ion

García et al. [34] showed that the decomposition of ampicillin is slow in the absence of Cd<sup>2+</sup> ion. Figure 7a shows the change of absorbance of ampicillin–AuNPs system in the presence and absence of Cd<sup>2+</sup> ion as a function of time.

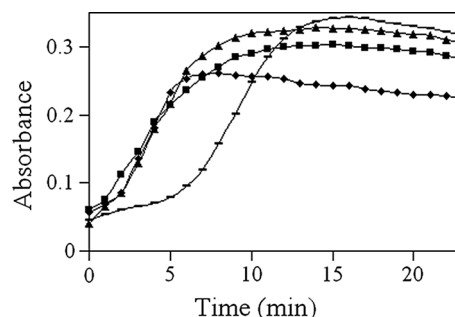


**Fig. 6** Effect of solvent on analytical signal. (black rectangle) H<sub>2</sub>O, (black triangle) Methanol, (black square) Ethanol, (black diamond) Propanol. Reaction conditions were pH 4.6, temperature 25 °C, C<sub>Amp</sub> = 56 μg ml<sup>-1</sup>, C<sub>Cd</sub><sup>2+</sup> = 5.0 × 10<sup>-4</sup> mol L<sup>-1</sup>

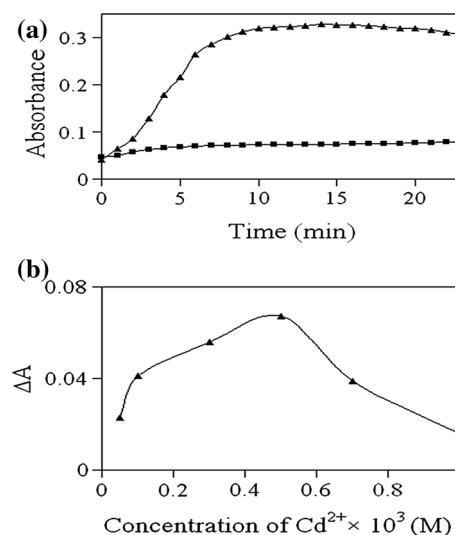


**Fig. 7 a** Absorbance changes of gold nanoparticles vs. time for (black triangle) catalyzed and (black square) non-catalyzed reaction by Cd<sup>2+</sup> ion, recorded at 670 nm. Reaction conditions were pH 4.6, temperature 25 °C, C<sub>Amp</sub> = 56 μg ml<sup>-1</sup>, C<sub>Cd</sub><sup>2+</sup> = 5.0 × 10<sup>-4</sup> mol L<sup>-1</sup>. **b** Effect of Cd<sup>2+</sup> concentration on analytical signal. Reaction conditions were pH 4.6, temperature 25 °C, C<sub>Amp</sub> = 56 μg ml<sup>-1</sup>

The effect of Cd<sup>2+</sup> on the reaction rate was also investigated in its concentration range of 5.0 × 10<sup>-5</sup>–1.0 × 10<sup>-3</sup> mol L<sup>-1</sup>. The results shown in Fig. 7b suggested an optimum concentration of 5.0 × 10<sup>-4</sup> mol L<sup>-1</sup> for Cd<sup>2+</sup>.

#### Effect of pH

The reaction rate and the stability of both ampicillin and gold nanoparticles are pH dependent; therefore, the maintenance of pH of the reaction mixture is critical. It should be mentioned that ampicillin is stable in the pH range of 3.5–6.0 [49]. Many researchers investigated the effect of pH on the aggregation of capped gold nanoparticles either

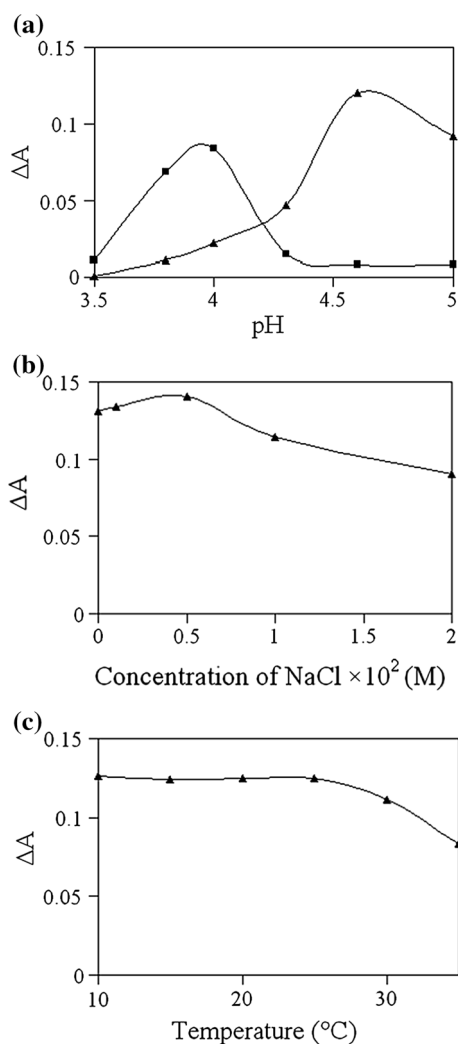


**Fig. 8** a Effect of pH on analytical signal in (black square) KHP and (black triangle) acetate buffers; b effect of ionic strength on analytical signal; c effect of temperature on analytical signal. Reaction conditions were  $C_{\text{Amp}} = 56 \mu\text{g ml}^{-1}$ ,  $C_{\text{Cd}^{2+}} = 5.0 \times 10^{-4} \text{ mol L}^{-1}$

**Table 1** Foreign ion study/selectivity on the determination of ampicillin trihydrate

Foreign ions or molecules	Tolerance level ( $\mu\text{g ml}^{-1}$ )
Glucose, galactose, fructose, sucrose	10
$\text{K}^+$	10
Sorbitol	5
$\text{Mg}^{2+}$	5
$\text{Ca}^{2+}$ , $\text{Zn}^{2+}$	3
Sodium citrate	1

in the presence or absence of other species [50]. To obtain a pH value corresponding to the optimum rate of reaction, the influence of pH on the decomposition rate of  $56 \mu\text{g ml}^{-1}$  ampicillin in the presence of  $5.0 \times 10^{-4} \text{ mol}$

$\text{L}^{-1} \text{ Cd}^{2+}$ , methanol as solvent and gold nanoparticles was studied in the pH range of 3.5–5.0 using different buffer solutions (acetate, potassium hydrogen phthalate, and citrate each with a concentration of  $0.05 \text{ mol L}^{-1}$ ). By using citrate buffer, even without adding ampicillin trihydrate, gold nanoparticles aggregate due to protonation of citrate. The results showed that in potassium hydrogen phthalate (KHP), the optimum pH was 4.0. In acetate buffer, with the same concentration as KHP, the optimum pH was found as 4.6 (Fig. 8a). However, with acetate buffer at pH 4.6, the change in absorbance was higher and consequently there was an improvement in sensitivity; this observation was also reported by other researchers. Therefore, acetate buffer with a pH of 4.6 was chosen for preparation of metal ion solution. It should be mentioned that at pH 4.6, which is the optimum pH in the proposed procedure for determination of ampicillin, the gold nanoparticles are still stable enough to be used as the spectroscopic probe reagent.

#### Effect of ionic strength

The effect of ionic strength on the rate of the reaction was studied using NaCl in the concentration range of 0.0 to  $2.0 \times 10^{-2} \text{ mol L}^{-1}$ . As the concentration of NaCl increased up to  $5.0 \times 10^{-3} \text{ mol L}^{-1}$ , the  $\Delta A$  value increased and eventually decreased. Sodium chloride with a concentration of  $5.0 \times 10^{-3} \text{ mol L}^{-1}$  provided a maximum change in  $\Delta A$  values (Fig. 8b). Hence, this concentration was considered for the next studies.

#### Effect of temperature

The effect of temperature was studied in the range of 10.0–35.0  $^{\circ}$ C. The results showed that the analytical signal was independent of temperature in the range of 10.0–25.0  $^{\circ}$ C (Fig. 8c). Eventually, a temperature of 25  $^{\circ}$ C was chosen as the optimum temperature.

#### Method validation

To show that this newly developed method is suitable for further use in determination of ampicillin, a validation study was performed according to the ICH guidelines [51]. In this regard, several parameters such as specificity, linearity, precision, accuracy, etc., were studied.

#### Foreign ion study/selectivity

Under the optimized experimental conditions, the influence of several coexisting foreign species with ampicillin was investigated for determination of  $56.0 \mu\text{g ml}^{-1}$  ampicillin. The maximum tolerable concentration of foreign species was taken when their concentration produced a change in

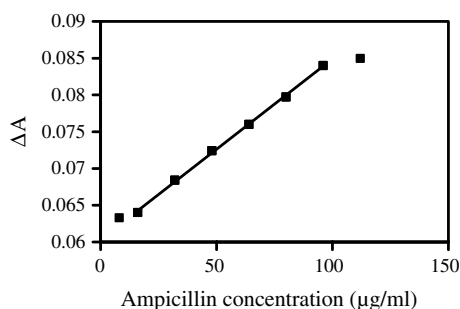


**Fig. 9** Calibration curve for ampicillin. Experimental conditions: acetate buffer with pH 4.6; temperature, 25 °C; and  $C_{Cd}^{2+} = 5.0 \times 10^{-4} \text{ mol L}^{-1}$

**Table 2** Optical and regression characteristics of ampicillin determination

Parameters	Results
$\lambda_{\text{max}}$	670 nm
Regression equation	$Y = 2 \times 10^{-4} C + 0.0603$
Correlation coefficient ( $R^2$ )	0.999
Linear dynamic range	16.0–96.0 $\mu\text{g ml}^{-1}$
Limit of detection	13.0 $\mu\text{g ml}^{-1}$
Relative standard deviation of mean ( $n = 10$ )	4.8 %
Variance	$1.36 \times 10^{-5}$
Standard deviation of slope	$2.25 \times 10^{-6}$
Standard deviation of intercept	0.0014

absorbance more than  $\pm 5\%$  of three replicate signal measurements for 56.0  $\mu\text{g ml}^{-1}$  ampicillin. As Table 1 shows, none of the foreign species which mostly are available in

**Table 3** Repeatability and intermediate precision of ampicillin determination

Concentration ( $\mu\text{g mL}^{-1}$ )	Repeatability ( $n = 3$ , intraday)		Intermediate precision ( $n = 3$ , interday)	
	Mean absorbance at 670 nm $\pm$ SD	% RSD	Mean absorbance at 670 nm $\pm$ SD	% RSD
25.0	0.0648 $\pm$ 0.0022	3.39	0.0644 $\pm$ 0.0024	3.72
40.0	0.0683 $\pm$ 0.0025	3.66	0.0677 $\pm$ 0.0029	4.28
60.0	0.0726 $\pm$ 0.0031	4.26	0.0721 $\pm$ 0.0034	4.71

**Table 4** Accuracy measurement for analysis of ampicillin showing recovery along with the standard deviation ( $n = 3$ )

Known concentration of ampicillin in original sample ( $\mu\text{g mL}^{-1}$ )	Excess ampicillin spiked (%)	Theoretical concentration ( $\mu\text{g mL}^{-1}$ )	Found concentration ( $\mu\text{g mL}^{-1}$ )	Recovery $\pm$ RSD
30.0	50	45.0	45.2 $\pm$ 2.2	100.4 $\pm$ 4.9
30.0	100	60.0	60.1 $\pm$ 2.7	100.9 $\pm$ 4.4
30.0	150	75.0	75.8 $\pm$ 3.5	101.0 $\pm$ 4.6

**Table 5** Determination of ampicillin in dosage form obtained from Dana, Farabi and Cosar pharmaceutical companies in Iran

Manufacturer	Claimed mg per capsule	Found mg $\pm$ SD per capsule
Dana pharmaceutical	500	508 $\pm$ 2
Farabi pharmaceutical	500	504 $\pm$ 2
Cosar pharmaceutical	500	496 $\pm$ 3

biological samples can significantly interfere for the ampicillin determination.

#### Analytical parameters and linearity

Under the optimum experimental conditions, the reaction was followed spectroscopically by measuring the absorbance as a function of time. Fixed time method was adopted for constructing the calibration curve. A linear relationship between  $\Delta A$  and the ampicillin concentration was obtained in the range of 16.0–96.0  $\mu\text{g ml}^{-1}$  ampicillin, with a regression equation of  $\Delta A = 2.0 \times 10^{-4} C + 0.0603$  with  $R^2 = 0.999$  (Fig. 9). The relative standard deviation for 10 replicate determinations of 56.0  $\mu\text{g ml}^{-1}$  ampicillin was 4.8 % and the detection limit [52] was found to be 13.0  $\mu\text{g ml}^{-1}$ . Table 2 shows the optical and regression characteristics of this method.

#### Precision

The repeatability (intraday) and intermediate precision (interday) were assessed by analyzing three different concentrations as 25, 40 and 60  $\mu\text{g mL}^{-1}$  of ampicillin. The results

**Table 6** Comparison of the proposed method with some spectrophotometric methods reported for ampicillin determination

Probe reagent	Wavelength (nm)	Linear range ( $\mu\text{g ml}^{-1}$ )	Detection limit ( $\mu\text{g ml}^{-1}$ )	References
Cu (II)	–	9.1–69.9	9.1	[53]
2,3-dichloro-5,6-dicyano-1,4-benzoquinone (DDQ)	524	$4.4 \times 10^2$ – $4.4 \times 10^3$	$1.6 \times 10^2$	[12]
Sodium hydroxide	268	20–100	–	[54]
Nickel chloride	265	3.5–55.8	2.6	[13]
Potassium peroxomonosulphate	302	1–50	1	[43]
Gold nanoparticles and cadmium (II)	670	16–96	13	This work

are summarized in Table 3. The % RSD values for precision suggested a good precision for this spectrophotometric assay.

#### Accuracy

Accuracy of the method was investigated using standard addition method at three concentrations of the standard solution. Standard quantity equivalent to 50, 100 and 150 % was added to the sample. Table 4 shows that the recoveries of the spiked drug were found to be 100.4–101.0 % indicating that this method was accurate.

#### Analysis of pharmaceutical formulations

The proposed procedure was applied for determination of ampicillin in dosage forms. For capsules analysis, three packs from three different series of ampicillin capsules were used. Table 5 summarizes the results obtained in the analysis of the pharmaceutical dosage. As shown in Table 5, the results of ampicillin analysis by proposed procedure provides good recoveries. It should be noted that other antibiotics that have lactam residue can behave like ampicillin and can be analyzed similarly.

#### Conclusion

The present study described kinetic-spectrophotometric method for the determination of ampicillin in pharmaceutical formulations with enhanced selectivity. The principal advantage of the proposed method was that the method was sensitive enough for analysis of lower amounts of ampicillin. Furthermore, the proposed method does not require expensive instruments and/or critical analytical reagents. A comparison between this work and some previously reported spectrophotometric techniques for determination of ampicillin is given in Table 6. As shown in this table, the linear dynamic range of this method is located in the trace concentration level and its detection limit is higher when compared with both Cu(II) and DDQ as probe reagents. Comparing to nickel chloride and potassium peroxomonosulphate, as probe reagents, the detection limit is lower but

the developed method provided a wider linear range. Moreover, ampicillin could be spectrophotometrically determined in the visible region (670 nm) so that the potential interference may be avoided and it does not suffer any positive or negative interference present in formulations.

**Acknowledgments** The authors wish to express their gratitude to Shiraz University Research Council for the support of this work.

#### References

- R. Hirsch, T.A. Ternes, K. Haberer, A. Mehlich, F. Ballwanz, K.L. Kratz, *J Chromatogr A* **815**, 213 (1998)
- T.L. Gilchrist, *Heterocyclic chemistry* (Longman Scientific, Harlow, 1987)
- A.A.P. Khan, A. Mohd, S. Bano, K.S. Siddiqi, A.M. Asiri, *Arabian J. Chem* (2012). doi:10.1016/j.arabjc.2012.04.033
- S.K. Sharma, L. Singh, S. Singh, *Sch. J. App. Med. Sci.* **1**, 291 (2013)
- J.L. Hope, K.J. Johnson, M.A. Cavelti, B.J. Prazen, J.W. Grate, R.E. Synovec, *Anal. Chim. Acta* **484**, 223 (2003)
- E. Verdon, R. Fuselier, D. Hurtaud-Pessel, P. Couedor, N. Cadieu, M. Laurentie, *J. Chromatogr. A* **882**, 135 (2000)
- F.A. Ibrahim, J.M. Nasr, *Anal. Methods* **6**, 1523 (2014)
- M.A. Badgujar, K.V. Mangaonkar, *Orient. J. Chem.* **27**, 1659 (2011)
- C. Venkatasamappa, P. Somanna, H. Sahajanda, *Int. J. Sci. Innov. Discov.* **4**, 71 (2014)
- L. Xu, H. Wang, Y. Xiao, *Spectrochim Acta Part A* **60**, 3007 (2004)
- A.S. Ahmad, N. Rahman, F. Islam, *J. Anal. Chem.* **59**, 119 (2004)
- C.C. Ezeanokete, K.G. Ngwoke, F.C. Okoye, P.O. Osadebe, *Eur. Chem. Bull.* **2**, 1009 (2013)
- I.R. Mišić, G. Miletić, S. Mitić, M. Mitić, E. Pecev-Marinković, *Chem. Pharm. Bull.* **61**, 913 (2013)
- M.A. Bacigalupo, G. Meroni, F. Secundo, R. Lelli, *Talanta* **77**, 126 (2008)
- C. Baraldi, A. Tinti, S. Ottani, M.C. Gamberini, *J. Pharm. Biomed. Anal.* **100**, 329 (2014)
- E.G. Tófoli, H.R.N. Salgado, *Phys. Chem.* **2**, 103 (2012)
- T.A.M. Msagati, M.M. Nindi, *Food Chem.* **100**, 836 (2007)
- C.S. Wu, J.L. Zhang, Y.L. Qiao, Y.L. Wang, Z.R. Chen, *Chin. Chem. Lett.* **22**, 334 (2011)
- M. Shamsipur, Z. Talebpour, H.R. Bijanzadeh, S. Tabatabaei, *J. Pharm. Biomed. Anal.* **30**, 1075 (2002)
- U.M. Reinscheid, *J. Pharm. Biomed. Anal.* **40**, 447 (2006)
- Y. Nia, Y. Wang, S. Kokot, *Talanta* **78**, 432 (2009)
- J.M. Calatayud, M.C. Icardo, *Encyclopedia of analytical science*, 2nd edn. (Elsevier, New York, 2005), pp. 373–383

23. X. Wei, L. Qi, J. Tan, R. Liu, F. Wang, *Anal. Chim. Acta* **671**, 80 (2010)
24. S. Guo, E. Wang, *Anal. Chim. Acta* **598**, 181 (2007)
25. M.M. Maye, L. Han, N.N. Kariuki, N.K. Ly, W.B. Chan, J. Luo, C.J. Zhong, *Anal. Chim. Acta* **496**, 17 (2003)
26. S. Bhattacharya, A. Srivastava, *Proc. Indian Acad. Sci. Chem. Sci.* **115**, 613 (2003)
27. N.G. Khlebtsov, L.A. Dykman, *J. Quant. Spectrosc. Rad. transf.* **111**, 1 (2010)
28. T. Kim, ChH Lee, S.W. Joo, K. Lee, *J. Colloid, Interf. Sci.* **318**, 238 (2008)
29. V. Myroshnychenko, J. Rodríguez-Fernández, I. Pastoriza-Santos, A.M. Funston, C. Novo, P. Mulvaney, L.M. Liz-Marzán, F.J. García de Abajo, *Chem. Soc. Rev.* **37**, 1792 (2008)
30. R. de la Rica, H. Matsui, *Chem. Soc. Rev.* **39**, 3499 (2010)
31. D. Aili, M.M. Stevens, *Chem. Soc. Rev.* **39**, 3358 (2010)
32. N.L. Rosi, C.A. Mirkin, *Chem. Rev.* **105**, 1547 (2005)
33. Z. Wang, L. Ma, *Coord. Chem. Rev.* **253**, 1607 (2009)
34. A.M. García, P.G. Navarro, P.J. Martínez, *Talanta* **46**, 101 (1998)
35. M.C. Daniel, D. Astruc, *Chem. Rev.* **104**, 293 (2004)
36. M. Green, *Chem. Commun.* **24**, 3002 (2005)
37. C.J. Murphy, T.K. Sau, A.M. Gole, C.J. Orendorff, J. Gao, L. Gou, S.E. Hunyadi, T. Li, *J. Phys. Chem. B* **109**, 13857 (2005)
38. Z.F. Zhang, H. Cui, M.J. Shi, *Phys. Chem. Chem. Phys.* **8**, 1017 (2006)
39. P. Li, L. Zhang, K. Ai, D. Li, X. Liu, E. Wang, *J. Control Release* **129**, 128 (2008)
40. S.A. Aromal, K.V. Dinesh Babu, D. Philip, *Spectrochim. Acta Part A* **96**, 1025 (2012)
41. W. Saul, K. Chan-Kyung, Y. Kiyull, *Can. J. Chem.* **72**, 1033 (1994)
42. M. Company, M.J. Benitez, J.S. Jiménez, *Int. J. Biol. Macromol.* **13**, 225 (1991)
43. S.P. Karpova, *J. Chem. Pharm. Res.* **5**, 57 (2013)
44. I.S. Lim, D. Mott, M.H. Engelhard, Y. Pan, S. Kamodia, J. Luo, P.N. Njoki, S. Zhou, L. Wang, C.J. Zhong, *Anal. Chem.* **81**, 689 (2009)
45. A. Mocanu, I. Cernica, G. Tomoaia, L.D. Bobos, O. Horovitz, M. Tomoaia-Cotisel, *Colloids Surf. A Physicochem Eng. Aspects* **338**, 93 (2009)
46. M.R. Hormozi-Nezhada, E. Seyedhosseini, H. Robotjazi, *Scientia Iranica F* **19**, 958 (2012)
47. V. Patil, R.B. Malvankar, M. Sastry, *Langmuir* **15**, 8197 (1999)
48. X.H. Zhang, S.F. Wang, *Sensors* **3**, 61 (2003)
49. US Pharmacopia, *The standard of quality*, 24th edn. (United Pharmacopia, USA, 2006), p. 166
50. I. Ojea-Jimenez, V. Puentes, *J. Am. Chem. Soc.* **131**, 13320 (2009)
51. ICH Harmonized Tripartite Guidelines, Validation of analytical procedures: text and methodology, Q2 (R), Nov 2005
52. J.N. Miller, J.C. Miller, *Statistics and chemometrics for analytical chemistry*, 5th edn. (England, Pearson Education Limited, 2005), pp. 121–124
53. A. Fernández-González, R. Badía, M.E. Díaz-García, *J. Pharm. Biomed. Anal.* **29**, 669 (2002)
54. H. Mahgoub, F. Ahmed Aly, *J. Pharm. Biomed. Anal.* **17**, 1273 (1998)